Journal of Hydrology 528 (2015) 668–682

Contents lists available at ScienceDirect

Journal of Hydrology

journal homepage: www.elsevier.com/locate/jhydrol

# On the hydrology of the bauxite oases, Cape York Peninsula, Australia

M. Leblanc [a,b,c,*], S. Tweed [a,b], B.J. Lyon [d], J. Bailey [b], C.E. Franklin [e], G. Harrington [f,g], A. Suckow [f,g]

[a] ANR Chair of Excellence, Research Institute for the Development (IRD), UMR G-EAU, 34000 Montpellier, France
[b] National Centre for Groundwater Research and Training (NCGRT) and Centre for Tropical Water & Aquatic Ecosystem Research (TropWATER), James Cook University, Cairns, Australia
[c] Laboratoire d'Hydrogéologie, UMR EMMAH, University of Avignon-INRA, Avignon, France
[d] Australia Zoo, Steve Irwin Wildlife Reserve, Australia
[e] School of Biological Sciences, The University of Queensland, Brisbane, QLD 4072, Australia
[f] CSIRO Land & Water, Gate 5 Waite Road, Urrbrae, SA 5064, Australia
[g] National Centre for Groundwater Research and Training (NCGRT), Flinders University, School of the Environment, Adelaide, Australia

ARTICLE INFO

*Article history:*
Received 12 August 2014
Received in revised form 12 May 2015
Accepted 1 June 2015
Available online 16 June 2015
This manuscript was handled by Laurent Charlet, Editor-in-Chief, with the assistance of Renduo Zhang, Associate Editor

*Keywords:*
Bauxite
Springs
Ecohydrology
Remote sensing
Hydrogeochemistry
Groundwater dating

SUMMARY

One of the world's largest bauxite deposits is located in the Cape York Peninsula, North-East Australia. Little is known about the hydrology of these remote bauxite deposits. Here, we present results from a multidisciplinary study that used remote sensing, hydrochemistry, and hydrodynamics to analyse the occurrence of several large oases in connection with the bauxite plateaus. Across this vast region, otherwise dominated by savannah, these oases are sustained by permanent springs and support rich and diverse new sub-ecosystems (spring forests) of high cultural values to the local indigenous population. The spring water chemistry reveals a well-mixed system with minor inter-spring variation; TDS values of spring waters are low (27–72 mg $L^{-1}$), major ion compositions are homogenous (Na–Si–DIC–Cl) and $\delta^{18}O$ and $\delta^{2}H$ values are reflective of rainwater origin with little evaporation prior to recharge. Dating of spring waters with anthropogenic trace gases (CFC-12 and $SF_6$) indicates mean groundwater residence times ranging from <1 to 30 years. An artificial tracing experiment highlighted the existence of a flow pathway from the bauxite land surface to the sandy aquifer that feeds the springs through discontinuities in the ferricrete layer. In addition, the soil infiltrability tests showed the bauxite land surface has very high infiltrability (15 mm $min^{-1}$), about four times greater than other adjacent land surfaces. Across the lower part of the Wenlock Basin, satellite data indicate a total number of 57 oases consistently located on the edge of the bauxite plateaus. This super-group of permanent hillslope springs and their ecosystems adds another important attribute to the list of natural and cultural values of the Cape York Peninsula.



## 1. Introduction

The early twentieth century saw the first extensive attempts by scientists to document and classify springs (Bryan, 1919; Meinzer, 1923). Many modern classification systems incorporate parts of early works and have expanded on these through the quantitative knowledge of springs (Alfaro and Wallace, 1994). There is however no widely accepted spring classification system with significance attributed to particular parameters, such as geologic origin, discharge, or chemical composition, and classification therefore remains subjective. In recent times the classification and description of springs has diversified from a primary focus on physical and chemical parameters (flow regime, hydrochemistry, and geologic setting) to become increasingly interested in the microclimates and ecosystems they support (Fensham et al., 2004; DWLBC, 2009; Springer and Stevens, 2009). The increased recognition of surface water and groundwater interactions in general, and spring fed streams and groundwater dependent ecosystems in particular, as having significant ecological implications has increased markedly over the last decade with the emergence of a new field known as hydroecology or ecohydrology (e.g. Hayashi and Rosenberry, 2002; Wood et al., 2008).

Management of springs and terrestrial groundwater dependent ecosystems (GDEs) requires, as a first step, the basin-scale mapping and characterisation of permanent spring waters. The mapping of GDEs in Australia has recently advanced though the development of The National Atlas of Groundwater Dependent Ecosystems, a comprehensive inventory of the location and characteristics of groundwater dependent ecosystems for Australia. It incorporates multiple lines of scientific evidence including

* Corresponding author at: Laboratoire d'Hydrogéologie, UMR EMMAH, University of Avignon-INRA, Avignon, France.
*E-mail address:* marc.leblanc@univ-avignon.fr (M. Leblanc).

http://dx.doi.org/10.1016/j.jhydrol.2015.06.001
0022-1694/

previous fieldwork, literature and mapping and products developed from analysis of remotely sensed data (SKM and CSIRO, 2012). Included in this Atlas are well-established Australian spring assemblages. For example the biodiversity and natural values associated with the springs of a large basin in central Australia, the Great Artesian Basin, are well-developed (Ponder, 1986; Fensham and Fairfax, 2003; Fensham and Price, 2004; Fensham et al., 2004, 2010). Threats from anthropogenic activities have also been identified (Ponder, 1986; Fensham, 1998; Mudd, 2000; Nevill et al., 2010). The conservation values of Great Artesian Basin springs is recognised in the Commonwealth Environment Protection and Biodiversity Conservation Act 1999 (EPBC Act) under the 'The community of native species dependent on natural discharge of groundwater from the Great Artesian Basin' listing (Department of the Environment, 2014).

However, there remain large areas in the remote northern regions of Australia where GDEs have not been identified or classified. To date, little is known about the hydrology and hydrogeology of the Cape York Peninsula; mostly due to a lack of *in-situ* observations in this remote region of northern Australia. In the Queensland Government database, only 44 springs are to date registered across the Cape York Peninsula (north of 16.5°S). For the Wenlock Basin, located in the north west of the Cape York Peninsula, two springs are registered in the upper part of the basin and none have been registered in the lower part. However, both local knowledge and the relatively high baseflow of the rivers compared with other regions of northern Australia (CSIRO, 2009), indicate that permanent springs are abundant in the landscape and play an active role in supporting surface waters and dependent ecosystems.

The Cape York Peninsula provides an ideal setting to explore hydroecological processes in their natural state. The region contains vast and relatively undisturbed landscapes, rich with Aboriginal traditions and customs, and high biological significance and diversity. For these reasons it is often considered for a nomination on the UNESCO World Heritage list (Valentine et al., 2013). Perennially flowing springs and watercourses in the Cape York Peninsula region support small assemblages of unique ecosystems within the wider savannah landscape. Unlike many areas of Australia, the freshwater-dependent ecosystems of Cape York Peninsula are relatively well-preserved and retain a high ecological integrity; possessing a diverse and unique array of aquatic, riparian and terrestrial biodiversity, near-natural flow regimes, and relatively intact riverine landscapes (Mackey et al., 2001; Kennard et al., 2010; Warfe et al., 2011; Valentine et al., 2013).

This paper investigates the permanent springs in the lower part of the Wenlock Basin, Cape York Peninsula. Due to little previous work on the hydrology of this remote region, in this study we undertake (1) a study of the spring occurrence; and (2) develop a first conceptual hydrodynamic and hydrochemical model of the springs. Firstly, the occurrence of these springs across the remote Wenlock Basin is determined using remote sensing data. The use of remote sensing techniques to map terrestrial GDEs is well-established (e.g. Boulton and Hancock, 2006; MacKay, 2006; Barquín and Scarsbrook, 2008; Howard and Merrifield, 2010). However, there has been a limited number of detailed studies worldwide focusing on the use of remote sensing to map spring waters (Saraf et al., 2000; Sener et al., 2005; Corsini et al., 2009; Oh et al., 2011). Here, we present an example of the use of remote sensing to detect the occurrence of springs in the remote Cape York Peninsula. During initial exploratory fieldwork 8 permanent spring systems were found and sampled in the lower Wenlock Basin (2 in the Ducie). These 8 surveyed springs systems served as ground truth for the satellite-based detection of additional new springs.

Secondly, chemistry and hydrodynamic data of surveyed springs are combined to determine the origins, chemical variability and flow pathways of the spring waters. This involves exploring the processes connecting the springs with the surrounding landscape, and in particular the springs' connectivity with nearby bauxite plateaus. This is achieved using a multi-disciplinary approach. To build a conceptual hydrodynamic and hydrochemical model of the springs we incorporate data from an artificial tracing experiment, soil infiltrability tests, stable isotope chemistry, major ion concentrations, and dating tracers; chlorofluorocarbons (CFC-12, CFC-11), sulphur hexafluoride ($SF_6$), and radiocarbon ($^{14}C$).

## 2. Study area

The study area, located in the north west of the Cape York bioregion, is formed by the lower part of the Wenlock Basin with its eastern boundary along the 142.5° longitude (Fig. 1). It is subject to a tropical savanna climate featuring high temperatures all year round, a short summer wet season, and a longer dry season between May and October, when little if any rain falls. Annual mean maximum and minimum temperatures for Weipa are 32.3 and 21.8 °C respectively. Mean annual rainfall is 2039 mm, and mean monthly rainfall for January and July is 484 and 1.6 mm respectively (Australian Bureau of Meteorology, 2014).

The bauxite land unit forms part of the broader Tertiary, Bulimba geological formation in western Cape York, which represents one of the largest areas of bauxite geology in the world (Willmott, 2009; Valentine et al., 2013). The study area includes the Steve Irwin Wildlife Reserve (SIWR) where the bauxite land unit occurs as a low, but distinctly elevated, plateau between 50 and 63 m (amsl). This bauxite plateau extends westward beyond the boundary of the SIWR. On the SIWR, the surrounding landscape to the plateau steadily grades downward to approximately 10 m (amsl) along the Wenlock River, to the south, south west, and south east and again towards the Ducie River to the north. A series of springs supporting lush oases flow from the margins of bauxite plateau at between 30 and 40 m elevation on the SIWR. These permanent springs are associated with a new sub-ecosystem type recently described by the Queensland Herbarium (Queensland Herbarium, 2014; Fig. 2): Regional Ecosystem Type 3.10.1.d: Springs and their vegetation communities (evergreen mesophyll/notophyll rainforest) associated with margins of Tertiary remnant plateaus on western Cape York. These ecosystems have been listed as "Of Concern" (QDEHP, 2014). These have been identified as having major ecological significance and performing vital ecological functions (Fell, 2009; Lyon and Franklin, 2012). Most of the plateau is vegetated by Regional Ecosystem Type 3.5.2, a tall Eucalypt woodland dominated by Darwin Stringybark *Eucalyptus tetradonta* (QDEHP, 2014). These woodlands are described as a unique Regional Ecosystem Type, being floristically distinct from the *Eucalyptus* formations in the Northern Territory (Specht et al., 1977), and representing the tallest structural development of *E. tetradonta* throughout tropical Australia (Sattler and Williams, 1999). A series of ephemeral, shallow swamps, largely vegetated by paperbark woodlands *Melaleuca* ssp. are situated towards the eastern end of the plateau, away from the areas of bauxite geology. Although not yet formally documented, the bauxite plateau and associated oases are known to be of major cultural significance to the Traditional Owners of the area, the Tephitthigghi people. Both the plateau and oases form part of tribal dreamtime stories, and it is believed the oases were birthing places for women (Arthur, 2009, pers. comm.).

## 3. Data and methods

In this study information from different disciplinary approaches were combined, including remote sensing data (Landsat 7 ETM+),

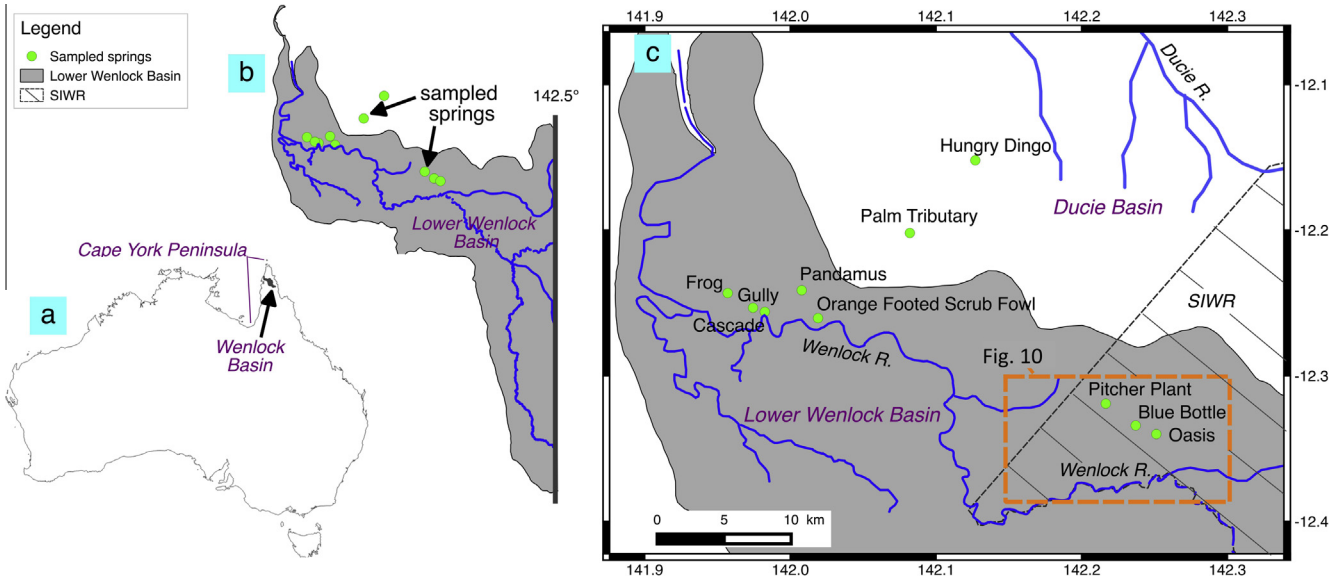


**Fig. 1.** Location map showing (a) the Wenlock Basin in Australia, (b) the lower part of the Wenlock Basin in grey shade (study area and extent of the remote sensing study) and (c) springs sampled for hydrochemistry and isotopic analyses (green dots). *SIWR* represents the boundary of the Steve Irwin Wildlife Reserve. (For interpretation of the references to colour in this figure legend, the reader is referred to the web version of this article.)

hydrochemical parameters (major ion, stable isotopes and dating tracers), and hydrodynamic data (hydraulic conductivity and tracing experiments) to analyse the characteristics and occurrence of the spring waters. These approaches, whilst not directly linked are complementary.

The remote sensing and hydrochemistry aspects of the paper both indicate different aspects of the spring system; the remote sensing is used to highlight the spring occurrence, whereas the chemistry is used to highlight the origin, chemical variability, and flow pathways of the spring waters. These two approaches, whilst not linked in their findings, both are useful in this remote and regional setting. We have aimed to emphasise this importance in the discussion and conclusions.

### 3.1. Remote sensing

8 new spring systems were found during initial fieldwork in the lower Wenlock Basin (Fig. 1, Section 4). Multispectral satellite imagery was used to map the possible occurrence of other previously un-reported spring systems across the lower Wenlock Basin using the 8 surveyed springs as ground truth.

#### (a) Selection of satellite data

In order to maximise the likelihood of effectively detecting springs through spectral indices the archives of Landsat 7 ETM+ imagery for the study area were searched to find the best combination of cloud-free, dry season imagery. The final mosaic is comprised of two Landsat ETM+ scenes acquired in August and September 2000 (Table 1). Both scenes were geometrically and radiometrically corrected with DN values converted to reflectance values using NASA LEDAPS atmospheric correction algorithm (Ju et al., 2012).

#### (b) Remote sensing indicator of oases

The Wenlock Basin receives extremely low rainfall in the dry season. In the dry tropics, remote sensing application to groundwater dependant ecosystems (GDE) studies is typically based around the premise that, if vegetation is very active, or wetlands and surface-water features persist, during dry periods they are likely to be using or containing water other than surface runoff or rain-fed infiltration. More generally, remote sensing can be used to detect areas where GDEs may occur. For example, time series of vegetation activity maps can be used to identify likely areas of groundwater discharge across large regions and to quantify the dynamics of associated wetlands (e.g. Petus et al., 2013).

The Normalised Difference Wetness Index (NDWI) is often used to map liquid water content of vegetation canopies from space (Gao, 1996). NDWI values can range from −1 (extremely dry) to 1 (extremely wet). To assess and ground truth the NDWI ability to distinguish the oases from the surrounding landscape, NDWI values at the location of the 8 surveyed springs in the lower Wenlock Basin (Fig. 1) were compared with that recorded at 1000 randomly generated points within the refined (masked) study area.

#### (c) Mask

The spring mapping methodology comprised applying a series of masks to the NDWI map of the region. Regional ecosystem type 3.5.4 is described as semideciduous notophyll vine forest occurring as small patches on northern plateaus. These areas return NDWI values consistent with the spring ecosystems. However previous investigations of these ecosystems in the vicinity of the Steve Irwin Wildlife Reserve failed to locate any springs (Lyon and Franklin, 2012). It is likely that these ecosystems are returning such high NDWI values due to a combination of their dense structure access and access to groundwater via their root system. It may seem counterintuitive to be masking GDEs however this exercise aimed to identify only springs rather than all GDEs. Additional masks were generated from ancillary data to exclude wetlands, gallery rainforest and estuarine vegetation from our analysis.

### 3.2. Hydrochemistry

Stable isotopes, major ions and dating tracers were analysed to characterise and identify controlling processes on spring water chemistry. In August/September 2011 and October/November 2012 (dry season) samples were collected from 10 different

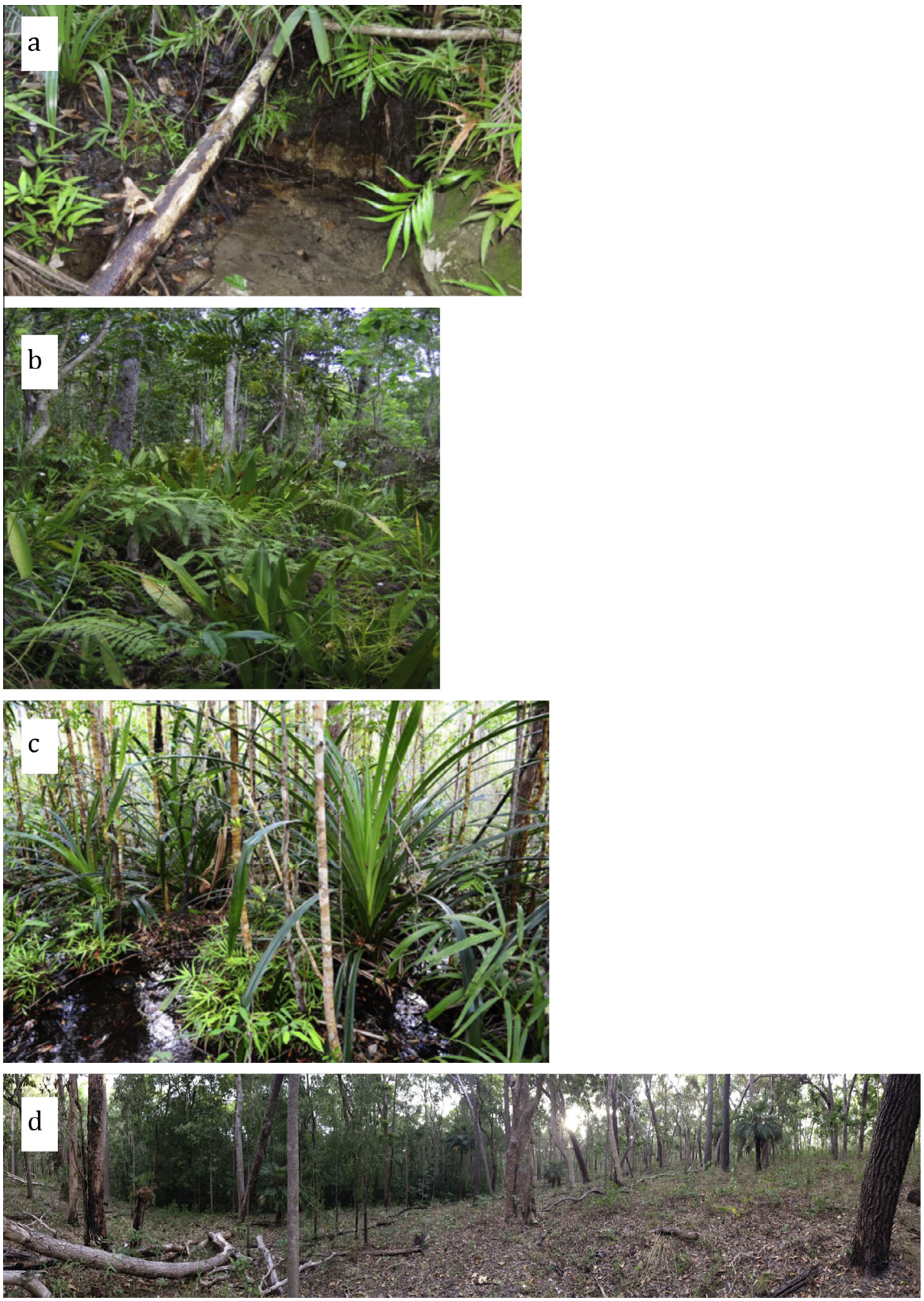


**Fig. 2.** Photographs of the bauxite oases taken in May and August 2014. (a) Spring water running over kaolin layer at Tentacle Spring. (b) Lush ground cover at Blue Bottle Spring. (c) Head of Oasis Spring with Callophyllum bicolor, a nationally threatened tree and (d) contrast between the spring forest (centre left) and the surrounding savannah vegetation.

springs. The samples were analysed for pH, temperature, total dissolved solids (TDS), major ion compositions, stable isotopes of water ($\delta^{18}O$ and $\delta^{2}H$), $\delta^{13}C_{DIC}$, radon-222 ($^{222}Rn$), chlorofluorocarbons (CFC-12, CFC-11), sulphur hexafluoride ($SF_6$), and radiocarbon ($^{14}C$). The locations of the spring sites sampled are presented in Fig. 1.

All samples were taken from flowing waters, and EC, pH and temperature were recorded in the field using a Thermo Scientific

**Table 1**
Details of the Landsat 7 ETM+ data selected for this study from USGS/EROS.

| Satellite sensor | Acquisition date | Path | Row | Cloud cover | Processing level | Scene ID |
|---|---|---|---|---|---|---|
| Landsat 7 ETM+ | 21/08/2000 | 98 | 69 | <10% | LEDAPS | SC20140317185959 |
| Landsat 7 ETM+ | 13/09/2000 | 99 | 68 | <10% | LEDAPS | LE70990682000257-SC20140316091136 |

Orion Star™ pH and conductivity meter. $HCO_3^-$ and dissolved $CO_2$ concentrations were also measured in the field using Hach digital titration kits. Detection limits for total alkalinity and dissolved $CO_2$ were 1.64 and 0.23 mM respectively, with precision of ~±10%. Replicates of $CO_2$ titrations revealed a poor reproducibility; therefore $CO_2$ and dissolved inorganic carbon (DIC) concentrations were calculated using the field measured pH, temperature and total alkalinity concentrations in the program CO2SYS (Lewis and Wallace, 1998). Samples in the field were also analysed for $^{222}Rn$ using a RAD7 meter (RAD $H_2O$ kit), and values were calibrated for temperature using the software Capture (Durridge).

The anion samples collected in the field were untreated, whereas samples for cation analyses were filtered (0.45 μm cellulose nitrate filter) and acidified to pH < 2 (ultrapure 16 N $HNO_3$) in the field. Cation and anion samples were analysed by ICP-OES and IC respectively at the CSIRO Analytical Services Unit.

Stable isotopes of water samples were analysed via mass spectrometry at the James Cook University Advanced Analytical Centre. Upon collection, spring water samples for $\delta^{13}C$ were frozen to prevent micro-organisms from altering the DIC isotope ratios.

The anthropogenic environmental tracers CFC-12, CFC-11 and $SF_6$ as well as $^{14}C$ were analysed in the spring waters. Samples of spring waters for CFC and $SF_6$ were collected in the field in glass bottles and were unfiltered. Collection involved using a metal bucket and the displacement method (following Oster et al., 1996). Samples were protected from possible atmospheric contamination by submersing the bottles under water. Four samples for CFCs (CFC-11 and CFC-12) and six samples for $SF_6$ were analysed at CSIRO Isotope Analysis Service. One sample for $^4He$ was collected in the field using a passive diffusion sampler following the method by (Gardner and Solomon, 2009). $^4He$ was also analysed at the CSIRO Isotope Analysis Service. Simulation models developed at the Leibniz Institute for Applied Geophysics (LIAG, Suckow, 2012) were used to interpret potential ranges in mean residence times (herein referred to as MRT) from the CFC and $SF_6$ concentrations, and are presented in the results section below. $^{14}C$ samples were analysed at the Australian National University Radiocarbon Dating Centre using a single stage accelerator mass spectrometer (Fallon et al., 2010).

It is generally accepted that groundwater, and especially springs where many flow lines converge, do not consist of one single scalar age but instead contain a whole distribution of different ages (Suckow, 2014). We therefore use tracer-tracer plots to indicate possible age distributions. The tracer-tracer plots for CFCs and $SF_6$ are based on maximum and minimum possible expected concentrations. Maximum concentrations occur under infiltration conditions with the lowest expected temperature (22 °C) and lowest altitude (40 m), and minimum concentrations under the highest temperature (30 °C) and highest altitude (150 m). Plots always use a pair of at least two tracers and indicate lines for three different age distribution scenarios. A piston flow model (PM) assumes no mixing along the flow pathway, whereas the exponential flow model (EM) assumes perfect groundwater mixtures, which also corresponds to a homogeneous aquifer with uniform areal recharge (Vogel, 1967). The Binary Mixing model (BM) assumes two component mixtures of modern water (recharged in 2012) with tracer-free old water (recharged prior to 1960 for CFCs and $SF_6$, more than 60ky ago for $^{14}C$). These scenarios are selected because they form boundary conditions that describe a space of all possible concentrations in the tracer-tracer plots: any mixing combination between these scenarios would lie in the space between the lines generated by the models.

### 3.3. Field saturated hydraulic conductivity

Field saturated hydraulic conductivity ($K_{fs}$), also often referred to as saturated soil infiltrability or infiltration capacity, defines the maximum rate at which water penetrates into the soil. It is controlled by soil factors alone and determined by the size, connectivity, orientation and stability (against wetting) of pores in soil, particularly the larger pores. Field saturated hydraulic conductivity is critical for determining runoff coefficient and infiltration (Bagarello et al., 2004; Cook, 2002).

The objective here is to estimate the infiltration capacity of the bauxite and to compare it with that of other land surface units in the area. There is no soil map for the study area, instead land surface units were classified into 5 groups according to the geology and geomorphology. Field saturated hydraulic conductivity of the soil was measured at 32 sites spread across these 5 land surface groups: (G1) laterite plateau covered by bauxite (10 sites); (G2) dark brown sandy clay soils with ironstone pebbles on top of laterite plateau without bauxite at surface, supporting seasonal swamps (5 sites); (G3) clayey sandy soils with ironstone pebbles on top of laterite plateau without bauxite at surface, supporting eucalypt woodlands (5 sites). G4 silt and clay grey soils above the Bulimba Formation/or Quaternary alluvial deposits (7 sites), G5 brown and yellow sandy loams soils above the Bulimba Formation, colluvial plain to gentle rise up to plateau (without bauxite) (5 sites).

A 'single-ring, falling head' method was used for measuring field-saturated hydraulic conductivity of the land surface. The method is a simplification of the twin-ring method (Cook, 2002). Infiltration rate is initially fast when the soil is dry, but then settles to a steady state. That 'steady-state' rate is the 'infiltrability or saturated infiltration rate'. Saturated infiltration rates were measured across the study area in September 2013 using steel rings of 200 mm in diameter and 170 mm in height with sharp edges on the side to penetrate the ground. 6 replicas were conducted at each site.

### 3.4. Tracing experiment

An artificial tracing experiment was conducted to test the hypothesis of a subsurface flow connection between the bauxite formation and the sandy aquifer beneath it. In ion-poor fresh environments such as our study area, diluted salt (NaCl) can be used for artificial tracing experiments (Kranjc, 1997; Goldscheider et al., 2008; Leibundgut et al., 2009). 50 kg of common salt (NaCl) was diluted in freshwater from the spring, and injected at once as a pulse on the land surface of the bauxite plateau near Oasis Spring on 13/2/2013. Location of the injection point was 12.338100°S and 142.253250°E, and was 220 m away from the head of Oasis Spring. Elevation difference between the injection point and the head of Oasis Spring is about 15 m. The concentration of the tracer was monitored in the downstream part of Oasis Spring where all the spring water converges to form a single stream (12.341389°S and 142.250833°E).

Electrical conductivity of the water offered an effective proxy to measure the tracer *in situ*. Two types of electrical conductivity (EC) measurements were performed. Before and after the tracing experiment EC was measured punctually using a portable field Orion Star™ conductivity meter (Thermo Scientific). During the tracing experiment, from 12/12/2012 to 07/08/2013, EC was monitored continuously at one-hour intervals using a CTD™ EC logger (Schlumberger) that was placed directly in the stream; the conductivity sensor of this logger is composed of platinum electrodes on ceramic ($Al_2O_3$) carrier. In both types of measurements, EC is compensated for temperature fluctuations and reported at 25 °C.

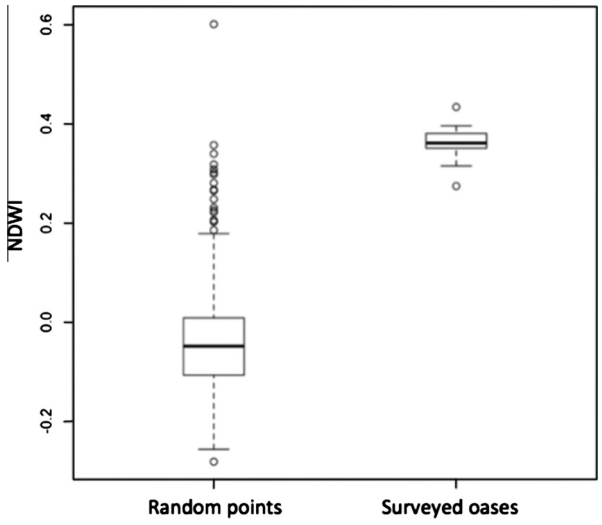


**Fig. 3.** NDWI values derived from Landsat reflectances for 1000 random points inside the study area (lower part of the Wenlock Basin) and the surveyed oases (Table 1).

## 4. Results

### 4.1. Remote sensing

Fig. 3 shows the high separability in Landsat NDWI values between the 8 surveyed oases (median = 0.36, SD = 0.04; location shown in Fig. 1) and the surrounding landscape represented by 1000 random points inside the study area (median = −0.05, SD = 0.09). A threshold value of 0.25 was applied to the Landsat NDWI to detect other potential oases across the entire study area excluding pockets of vine forests, gallery rainforests, wetlands, and estuarine vegetation (see masking in Section 3.5). Fig. 4 shows an example of the results from this mapping exercise. Surveyed oases, shown as green dots, are characterised by high NDWI values and are in sharp contrast with the surrounding landscape. More potential oases, highlighted as purple circles in the figure, are captured by the NDWI map. Across the lower part of the Wenlock Basin, this technique indicates a total number of 57 oases including the 8 surveyed and sampled in the field. The largest oasis detected, ~22 ha, is located at 12.235°S and 142.140°E. Bluebottle Oasis (~12.5 ha), on the Steve Irwin Wildlife Reserve, is the second largest oasis found in the lower Wenlock Basin.

A remarkable concentration of 45 oases is found in an area between 12.200°S–141.950°E and 12.350°S–144.320°E (average density ~1 oasis per 4 $km^2$). This oases 'hot spot' includes the SIWR and the bauxite plateau to the east of it. Another smaller

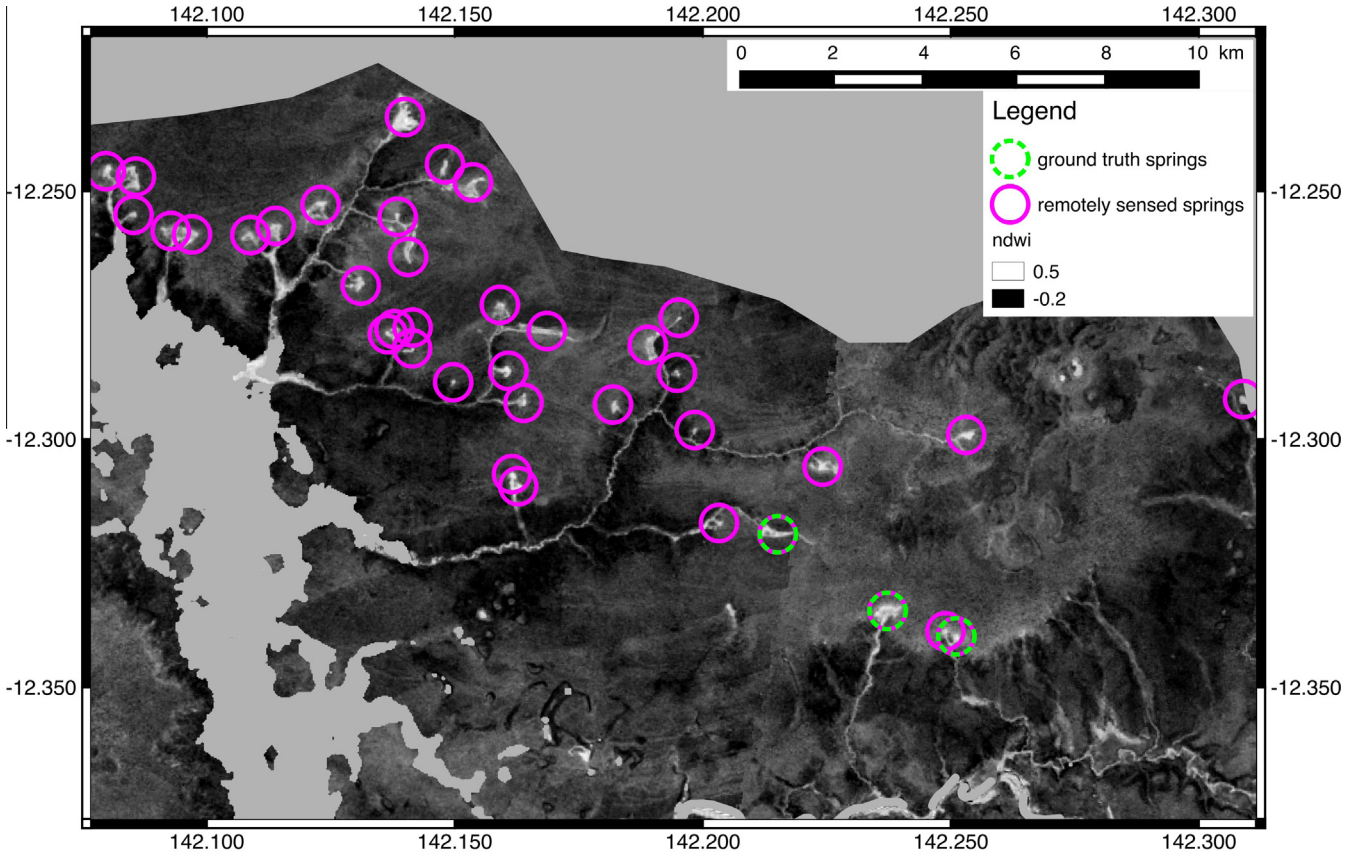


**Fig. 4.** Map showing an example of the NDWI distribution in the lower Wenlock Basin during the dry season, the surveyed ground truth oases (green circles) and the NDWI-detected oases (purple circles). (For interpretation of the references to colour in this figure legend, the reader is referred to the web version of this article.)

'hot spot' of ~25 km$^2$ and composed of 9 oases is found between 12.470°S–142.240°E and 12.520°S–142.340°E. An overlay of the mapped oases and of the geology (Fig. 5) shows there is a strong spatial correlation between the occurrence of oases and the edges of the bauxite plateaus.

### 4.2. Hydrochemistry

Results from the stable isotope analysis show that the spring $\delta^2$H and $\delta^{18}$O isotope values are close to rainfall values of the global meteoric water line (GMWL) and the Cairns MWL, which indicates a meteoric origin of the spring waters (Fig. 6). The $\delta^2$H and $\delta^{18}$O values can also be used to indicate effects of evaporation, which can result in an increase in TDS values. The spring water $\delta^2$H and $\delta^{18}$O values close to the meteoric water lines indicate little or no evaporation affects. Spring samples plot in a narrow cluster (−5.8‰ to −7.7‰ and −38‰ to −49‰ in $^{18}$O and $^2$H respectively) compared to the rain water samples. This indicates considerable mixing of the rainfall events recharging the spring system. Repeated sampling of Oasis Spring does highlight some temporal difference in the $\delta^2$H and $\delta^{18}$O values. Between the dry season (August) values in 2011 compared with dry season (October) values sampled the following year (2012), $\delta^2$H and $\delta^{18}$O values increase by 1.3‰ and 5.2‰ respectively (Table 2).

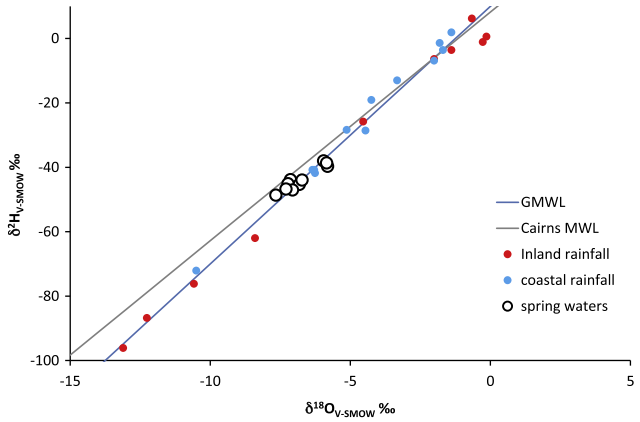


**Fig. 6.** Stable isotope values of spring waters, compared with the Global Meteoric Water Line (GMWL), the Cairns meteoric water line (MWL; Munksgaard et al., 2012), and rainfall values from a coastal (Darwin) and inland (Mt Isa) site (Crosbie et al., 2012).

The spring waters have low pH values ranging from 4.61 to 5.15 (Table 2) and the major ion concentrations suggest that there is limited mineral dissolution occurring along groundwater flow pathways to these springs. The TDS concentrations of spring

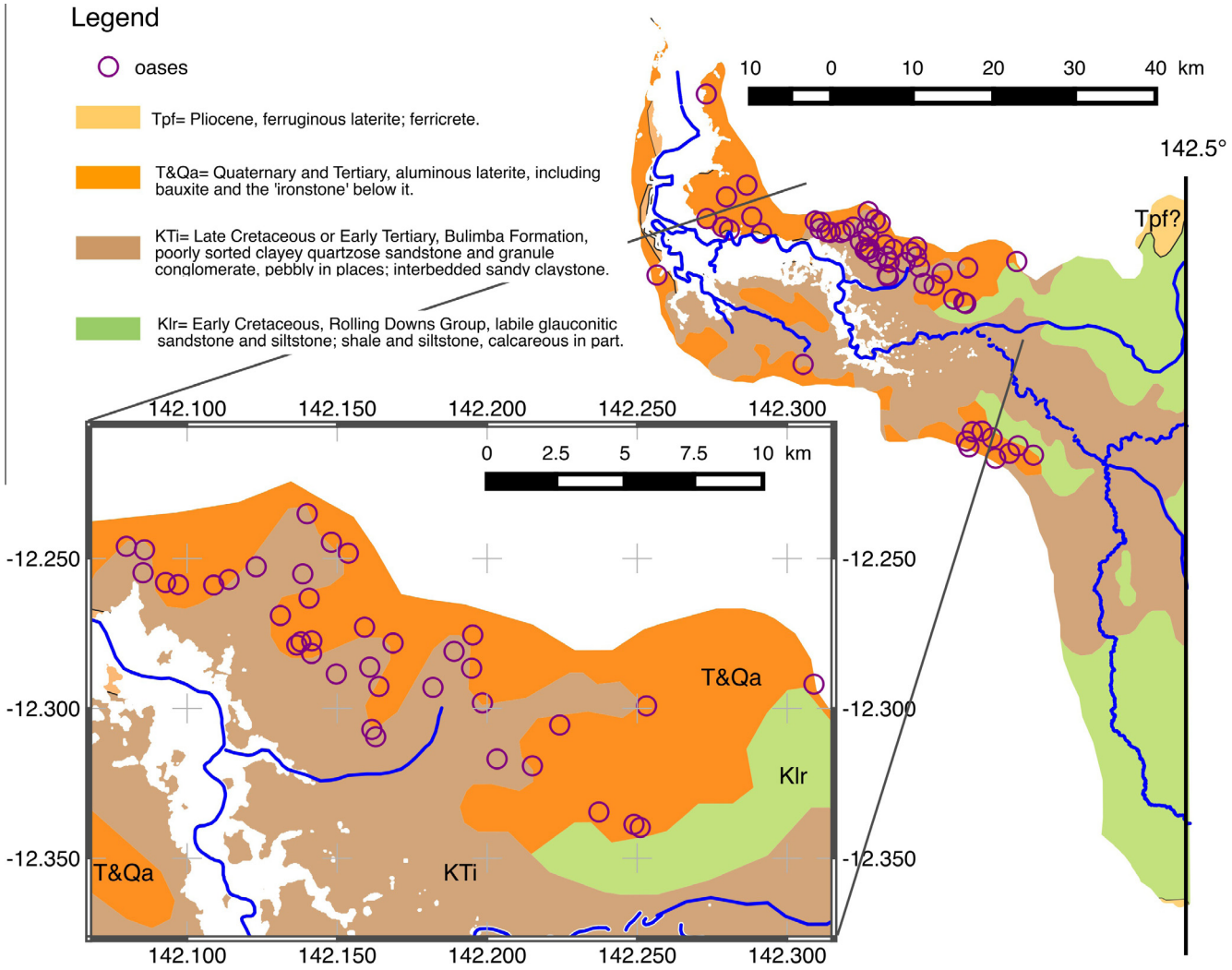


**Fig. 5.** Map showing the geology of the area and the distribution of the detected oases. Rock description from the 1:250,000 geology map, Weipa sheet SD54-3.

**Table 2**
Results of field parameters, major ions, stable isotopes and $^{222}Rn$ for the spring waters.

| Sample ID | Lat | Long | pH | Temp (°C) | DO (mg/L) | $CO_2$ (mg/L | $F^-$ (mg/L) | $Cl^-$ (mg/L) | $Br^-$ (mg/L) | $NO_3^-$ (mg/L) | $SO_4^{2-}$ (mg/L) | $Ca^{2+}$ (mg/L) | $K^+$ (mg/L) | $Mg^{2+}$ (mg/L) | $Na^+$ (mg/L) | Si (mg/L) | TDS (mg/L) | $\delta^{18}O$ (‰) | $\delta^2H$ (‰) | $\delta^{13}C_{DIC}$ (‰) | $^{222}Rn$[a] (Bq/L) |
|---|---|---|---|---|---|---|---|---|---|---|---|---|---|---|---|---|---|---|---|---|---|
| *Sampled August 2011* | | | | | | | | | | | | | | | | | | | | | |
| Blue Bottle Spring | −12.334 | 142.237 | 4.88 | 28.5 | 6.0 | 16.13 | <0.05 | – | <0.05 | <0.05 | 0.87 | <0.1 | <0.1 | 0.33 | 2.56 | 2.43 | – | −5.95 | −38.00 | −21.66 | 7.7 ± 3 |
| Pitcher Plant Spring | −12.321 | 142.223 | 5.14 | 26.3 | – | 14.88 | <0.05 | 4.7 | <0.05 | <0.05 | 0.10 | <0.1 | <0.1 | 0.45 | 2.56 | 2.18 | 28.6 | −5.81 | −39.71 | −12.73 | 33.1 ± 6 |
| Oasis Spring | −12.339 | 142.252 | 4.87 | 28.1 | 8.0 | 21.35 | <0.05 | 5.2 | <0.05 | <0.05 | 0.11 | <0.1 | <0.1 | 0.43 | 2.90 | 2.65 | 35.6 | −5.84 | −38.63 | −19.77 | 15.2 ± 4 |
| *Sampled October 2012* | | | | | | | | | | | | | | | | | | | | | |
| Oasis Spring | −12.339 | 142.252 | 4.92 | 27.2 | 4.7 | 18.28 | – | – | – | – | – | <0.1 | <0.1 | 0.46 | 3.45 | 2.53 | | −7.13 | −43.84 | – | – |
| Frog | −12.244 | 141.957 | 4.96 | 24.9 | 3.3 | 17.19 | <0.05 | 4.5 | <0.05 | <0.05 | 0.20 | <0.1 | <0.1 | 0.33 | 2.45 | 2.22 | 29.8 | −7.15 | −46.56 | – | 5.9 ± 3.3 |
| Cascade | −12.257 | 141.982 | 4.61 | 28.8 | 4.1 | 44.12 | <0.05 | 4.6 | <0.05 | <0.05 | 0.15 | <0.1 | <0.1 | 0.34 | 2.60 | 2.41 | 57.7 | −7.22 | −45.09 | – | 2.4 ± 1.3 |
| Gully | −12.253 | 141.976 | 4.61 | 27.4 | 0.5 | 52.42 | <0.05 | 4.5 | <0.05 | <0.05 | 0.11 | <0.1 | <0.1 | 0.37 | 2.45 | 2.22 | 66.1 | −7.65 | −48.65 | – | 18.0 ± 3.2 |
| Orange footed scrub fowl | −12.259 | 142.019 | 5.14 | 27.6 | 6.4 | 12.81 | <0.05 | 5.2 | <0.05 | <0.05 | 0.10 | <0.1 | <0.1 | 0.41 | 2.39 | 2.40 | 26.5 | −6.82 | −45.30 | – | 2.6 ± 1.4 |
| Hungry dingo spring | −12.153 | 142.126 | 5.15 | 28.6 | 5.6 | 11.28 | <0.05 | 6.1 | <0.05 | <0.05 | 0.15 | 0.12 | 0.30 | 0.57 | 3.69 | 2.51 | 27.7 | −6.72 | −43.95 | – | 1.4 ± 1.1 |
| Pandamus | −12.241 | 142.008 | 4.61 | 27.4 | 1.3 | 57.63 | <0.05 | 4.9 | <0.05 | 0.32 | 0.10 | <0.1 | <0.1 | 0.31 | 2.27 | 2.29 | 72.3 | −7.06 | −47.04 | – | 18.5 ± 5.2 |
| Palm tributary | −12.203 | 142.083 | 4.78 | 27.0 | 1.5 | 26.51 | <0.05 | 4.3 | <0.05 | 0.05 | 0.06 | 0.35 | <0.1 | 0.44 | 2.24 | 2.20 | 39.2 | −7.30 | −46.76 | – | 14.3 ± 3.4 |

[a] Range of uncertainty (±) calculated from the corrected average of 2-Sigma Uncert (Bq/L).

waters range from 27.7 to 72.3 mg $L^{-1}$ and are dominated by Na–Si relative to Mg (Si is present as $H_4SiO_4$ for this pH range; Langmuir, 1997) and DIC–Cl relative to $SO_4$ (DIC is mostly present as $CO_2$ for this pH range; Drever, 1997) (Fig. 7). Local rainfall compositions were not available at the study site, however rainfall chemistry from northern Australian coastal (Townsville and Darwin) and

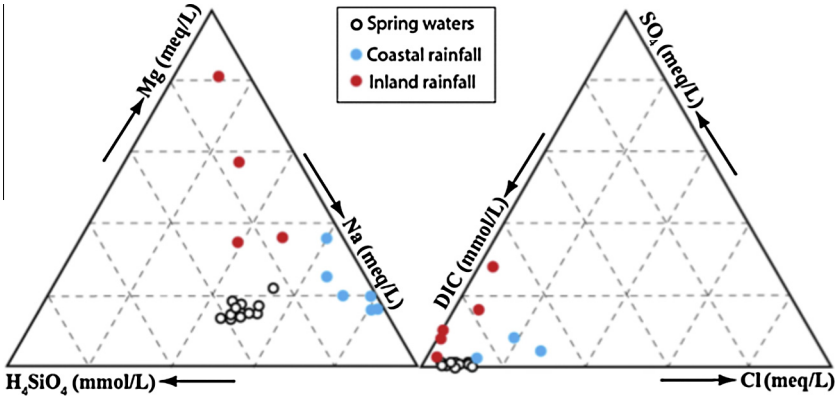


**Fig. 7.** Ternary plot of Mg, Na, and $H_4SiO_4$, and $SO_4$, Cl and DIC concentrations in spring waters, in comparison with ranges in rainfall data from coastal rainfall (Darwin and Townsville) and inland rainfall (Mt Isa) in northern Australia (rainfall data from Crosbie et al., 2012).

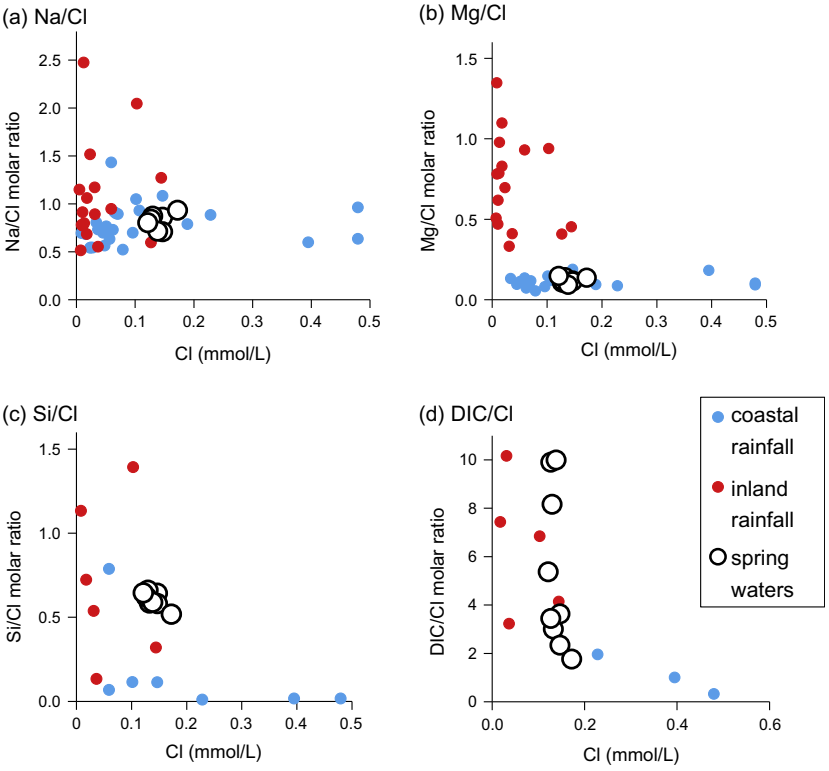


**Fig. 8.** Spring water Na/Cl, Mg/Cl, Si/Cl, and DIC/Cl molar ratios in comparison with ranges in rainfall data from coastal rainfall (Darwin and Townsville) and inland rainfall (Mt Isa) in northern Australia (rainfall data from Crosbie et al., 2012).

**Table 3**
Concentrations of SF6, CFC-11, CFC-12, terrigenic $^4$He and $^{14}$C of spring waters.

| Spring name | Date | SF6 | CFC-11 | | CFC-12 | | Terrigenic $^4$He | Percent modern |
|---|---|---|---|---|---|---|---|---|
| | | fMol/L | pmol/kg | ± | pmol/kg | ± | cc/g | carbon (pMC) |
| Blue Bottle | 26-August-11 | 0.92 | 0.70 | 0.08 | 1.11 | 0.06 | | 110 |
| Pitcher Plant | 27-August-11 | 1.83 | 2.64 | 0.12 | 1.55 | 0.04 | | 108 |
| Oasis | 27-August-11 | 1.28 | 1.49 | 0.11 | 1.23 | 0.04 | 4.98E−08 | |
| Hungry dingo | 16-October-12 | 1.49 | 1.61 | 0.02 | 1.18 | 0.04 | | |
| Pandamus | 17-October-12 | 1.44 | | | | | | |
| Palm tributary | 17-October-12 | 1.55 | | | | | | |

inland (Mt Isa) sites (Crosbie et al., 2012) are compared with the spring waters in Fig. 3. Similar to the stable isotope results, the relative concentrations of the major ions in spring waters compared to rainfall generally reflect a more homogenous composition and have values ranging in between the coastal and inland rainfall chemical compositions.

Dominant ions are presented relative to Cl (Fig. 8); to analyse the increases in ion concentrations relative to rainfall chemistry, and exclude the effects of evapotranspiration. The molar ratios of Na/Cl (0.71–0.93) and Mg/Cl (0.09–0.15) for the spring waters show no significant increases in Na or Mg concentrations relative to Cl above atmospheric inputs that would indicate additions from water-rock interactions (Fig. 8a and b). The Si concentrations may increase due to mineral weathering reactions, resulting in relatively high Si/Cl molar ratios (0.52–0.64; Fig. 8c). However this also depends on the local rainfall composition. Rainfall compositions show that the ion ratios of inland rainfall can have large variations in Si/Cl molar ratios (0.13–1.39).

DIC/Cl molar ratios of spring waters (3.01–10.00) are also high compared with coastal rainfall and are within the range indicated

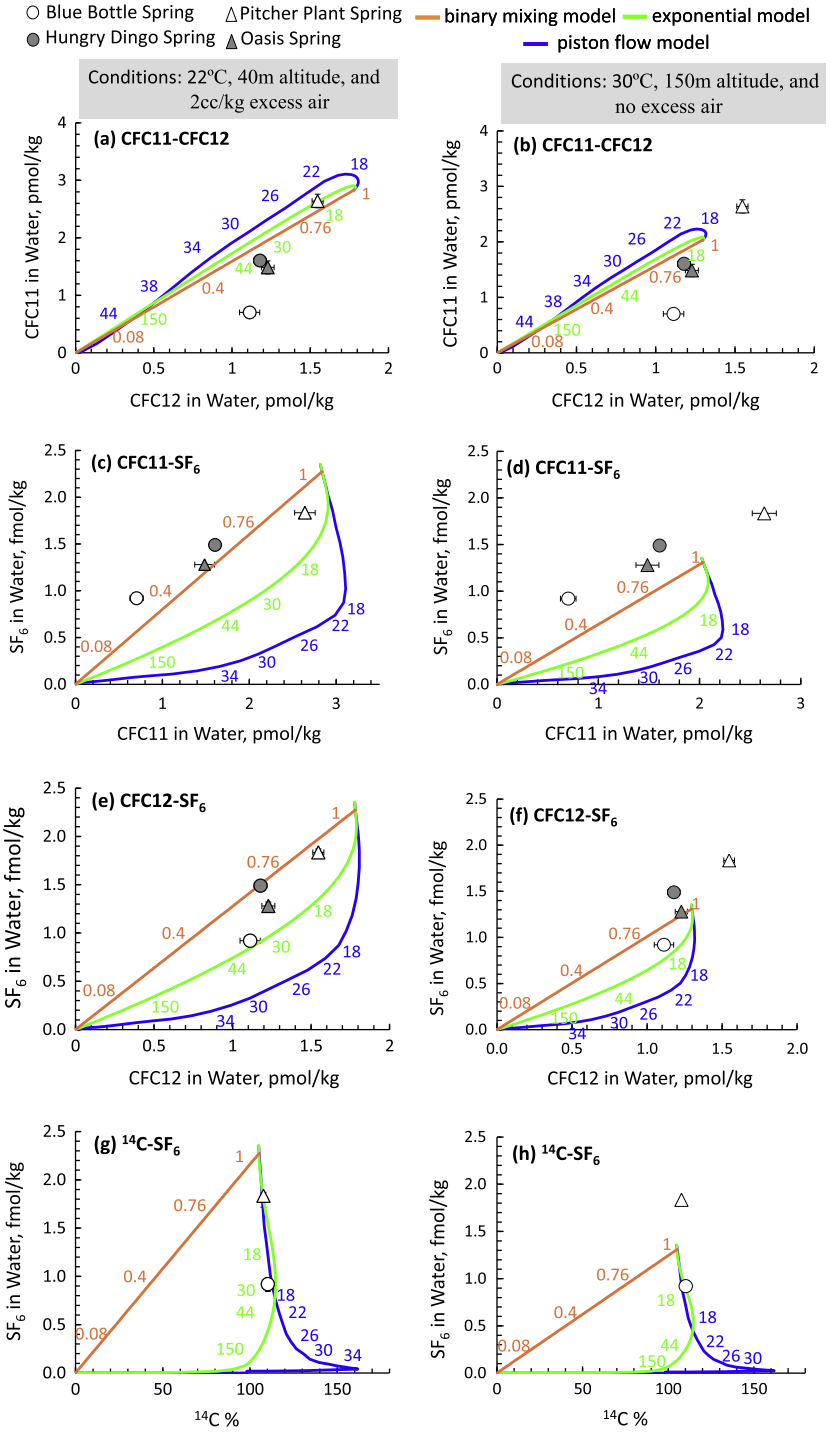


**Fig. 9.** Age dating tracers as tracer-tracer pairs with lines of binary mixing, piston flow and exponential models. Left column indicates infiltration conditions of 22 °C, 40 m altitude and 2 cc/kg excess air. Right column indicates conditions of 30 °C, 150 m altitude and no excess air. Only the scenarios in the left column can explain all data points, if degradation of CFCs is taken into account. See text for further explanations.

by inland rainfall chemistry (Fig. 8d). Additional sources of DIC in the system (other than atmospheric) can be derived from respired soil $CO_2$ from the C3 or C4 plants and dissolution of freshwater carbonates (e.g. Schulte et al., 2011). For the spring waters, only three samples were analysed for $\delta^{13}C_{DIC}$, and values range from −12.73‰ at Pitcher Plant spring, to −19.77 and −21.66‰ at Oasis and Blue Bottle Springs respectively (Table 2). These values can represent a mix of DIC from the different sources, and further sampling of $\delta^{13}C_{DIC}$ would be required to analyse the origins of DIC in this spring water system.

### 4.3. Spring water dating

The results of $SF_6$ and CFCs are presented in Table 3. The $SF_6$ concentrations range from 0.92 to 1.83 fMol $L^{-1}$, with highest concentrations observed at Pitcher Plant spring and lowest concentrations observed at Blue Bottle spring (Table 3). The CFC-11 and CFC-12 concentrations also show highest values recorded at Pitcher Plant spring (2.64 and 1.55 pmol/kg respectively), and lowest values recorded at Blue Bottle spring (0.70 and 1.11 pmol/kg respectively) (Fig. 9a). On two of the springs (Blue Bottle and Pitcher Plant) $^{14}C$ activity of DIC was also measured and gave post-modern values higher than 100 pMC (Table 3). Helium, Neon and Argon measured on Oasis Spring gave values that can be explained by solubility equilibrium at 20–25 °C and less than 2 cc/kg excess air (Heaton and Vogel, 1981). These values do not contain any terrigenic helium component, which would indicate old water (Torgersen and Stute, 2013). Therefore all age indicating tracers show that either all the investigated spring waters are younger than 1963 or that they at least contain a large component of such water, and that none of the tracers measured give indications of water components recharge prior to 1960.

The plotted concentrations of CFC-11 indicate there is CFC-11 degradation occurring, which is likely to be due to anaerobic microbial degradation (Plummer and Busenberg, 1999; Darling et al., 2012) (Fig. 9). We exclude contamination of CFC-12 due to the remoteness of the area from anthropogenic contamination sources and because none of the samples indicate concentrations outside of the range expected for clean air and the possible infiltration conditions. Sorption of CFCs can also result in decreased CFC concentrations where there is a high organic matter content in the matrix (IAEA, 2006). CFC-12 is generally assumed to be more stable than CFC-11 and degrading a factor of 10 slower. But only one study tried to quantify this ratio systematically (Oster et al., 1996) and it may vary depending on geochemical conditions. Therefore degradation of CFC-12 cannot be excluded. Degradation of $SF_6$ has not yet been reported in the literature. In this study, the degradation of CFC-11 is indicated by a shift of data points downward in comparison to the model lines in Fig. 9a and b and to the left in Fig. 9c and d. Degradation of CFC-12 in the sampled springs is indicated by a shift of data points to the left in Fig. 9e and f.

### 4.4. Field saturated hydraulic conductivity

The results are shown for each of the five land surface units encountered (Fig. 10 and Table 4). $K_{fs}$ of the bauxite land surface was measured at 9 sites (54 measurements) and ranges from 7.6 to 34.4 mm $min^{-1}$. Fig. 11 indicates that $K_{fs}$ of the bauxite land surface is significantly higher than that of the other soil types encountered. On the laterite plateau, the median $K_{fs}$ of the bauxite land surface is ~5 times higher than that of swamp soils and ~4 times higher than that of the clayey sandy soils of the woodlands.

### 4.5. Tracing experiment

Results from the tracing experiment are shown in Fig. 12. Time series of EC recorded at the spring show an important and

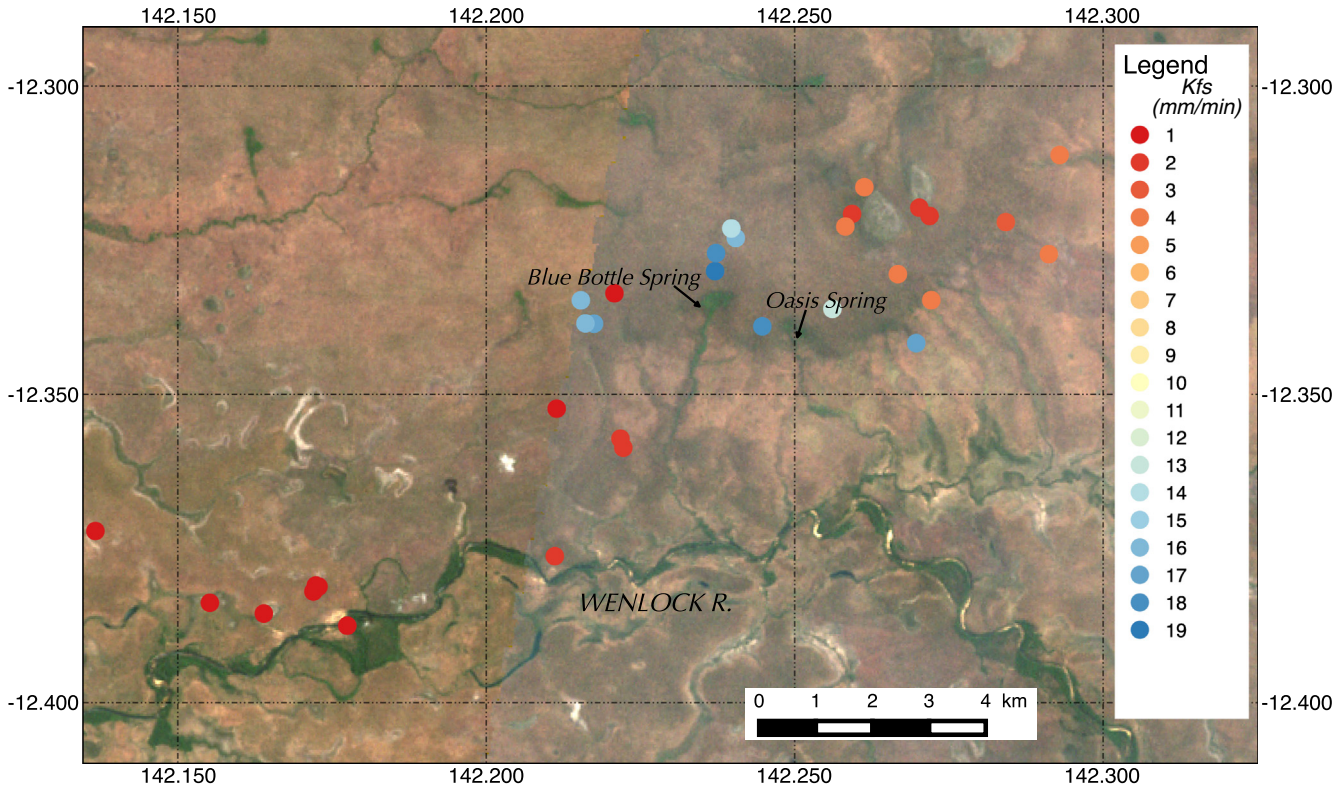


**Fig. 10.** Map showing the spatial distribution of the soil infiltrability values. Location of the surveyed area is also shown in Fig. 1.

**Table 4**
Field saturated hydraulic conductivity values ($K_{fs}$) for each soil type in mm min$^{-1}$.

| Group | Min., $K_{fs}$ | 1st Qu., $K_{fs}$ | Median, $K_{fs}$ | Mean, $K_{fs}$ | 3rd Qu., $K_{fs}$ | Max., $K_{fs}$ | Nb sites | Nb measures (6 replicates) |
|---|---|---|---|---|---|---|---|---|
| 1 | 7.60 | 11.95 | 14.85 | 16.28 | 18.62 | 34.40 | 9 | 54 |
| 2 | 1.40 | 2.45 | 2.90 | 3.17 | 3.57 | 6.60 | 5 | 30 |
| 3 | 2.90 | 3.90 | 4.00 | 4.01 | 4.27 | 4.90 | 5 | 30 |
| 4 | 0.70 | 1.10 | 1.20 | 1.14 | 1.30 | 1.40 | 7 | 42 |
| 5 | 0.80 | 1.17 | 1.65 | 1.83 | 2.20 | 5.00 | 5 | 30 |

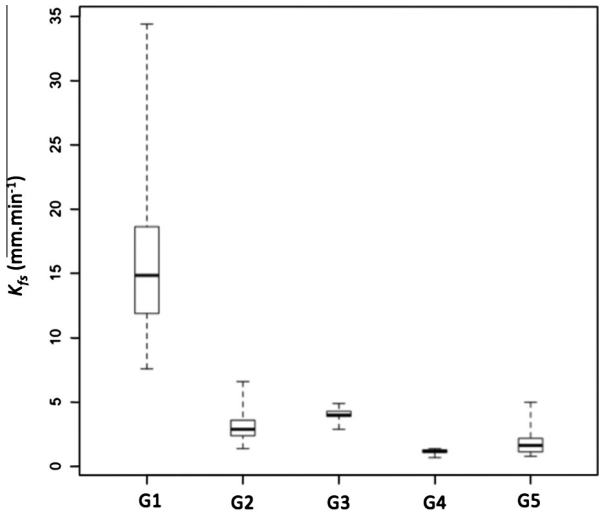


**Fig. 11.** Whisker plots showing the distribution of the infiltration values for each soil type (min, 25th percentile, median, 75th percentile, max). (G1) Aluminous laterite plateau covered by bauxite in the surface layer (sites 11–20); (G2) aluminous laterite plateau without bauxite at surface. Dark brown sandy clay soils with integrated ironstone pebbles supporting paperbark seasonal swamps (sites 1–5); (G3) aluminous laterite plateau without bauxite at surface. Clayey sandy soils with integrated ironstone pebbles supporting eucalypt woodlands (Darwin Stringybark) (sites 6–10). (G4) Silt and clay grey soils above the Bulimba Formation/or Quaternary alluvial deposits (sites 21–27), (G5) Brown and yellow sandy loams soils above the Bulimba Formation (EAST). Adjacent to the Straight – Colluvial plain to gentle rise up to Plateau (NOT bauxite geology) (sites 28–32).

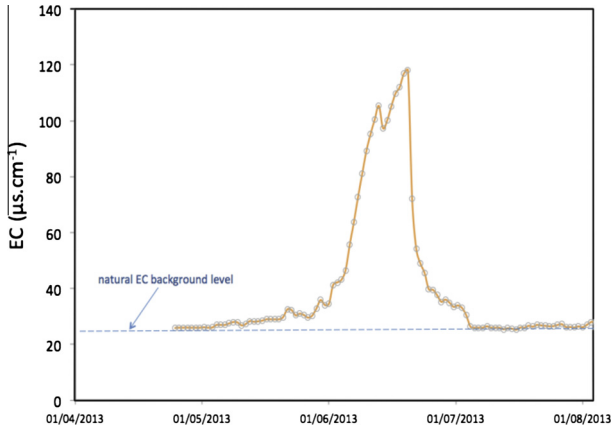


**Fig. 12.** Tracing experiment from the bauxite plateau to Oasis Spring. Daily specific conductivity (EC at 25 °C) logged *in situ* in the downstream part of Oasis Spring.

prolonged rise of the water mineralisation, well above the natural background level (25 µS cm$^{-1}$), which is indicative of the tracer plume. The first quartile of the tracer (25%) arrived at the spring on 09/06/2013; 116 days after injection. The tracer concentration (as recorded by EC) peaked on 20/06/2013 at 120 µs cm$^{-1}$. The median residence time of the tracer in the environment before reaching Oasis Spring was of 122 days. This equates to a median velocity of the tracer of ~1.8 m d$^{-1}$ (10th percentile ~2 m d$^{-1}$; 90th percentile ~1.6 m d$^{-1}$). Thus, the tracer was not carried by surface runoff or subsurface pipeflow/interflow. Rather, the tracer velocity is characteristic of porous media. Assuming a hydraulic gradient of 0.068 (considering elevation difference and distance from injection point to spring given in Section 3.4) and an effective porosity ranging from 5% to 15%, the median velocity indicates a hydraulic conductivity from 1.3 to 4.0 m d$^{-1}$, which is typical for fine to medium sands (Domenico and Schwartz, 1990).

This tracing experiment demonstrates the existence of a substantial groundwater flow path from the bauxite land surface to the sandy aquifer and Oasis Spring through discontinuities in the ferricrete ironstone (Fig. 13). It also is an independent indication that a continuous age distribution is more probable to explain the combined findings of the tracer test and of the CFC/$SF_6$ data than a simple piston flow approach (Fig. 13).

## 5. Discussion

### 5.1. Spring occurrence

There is a demonstrated potential for utilising remotely sensed multispectral data in conjunction with field surveys to characterise the nature and spatial distribution of GDEs across an entire landscape. This information and methodology can potentially be of great use in the assessment and management of natural resources particularly in remote, inaccessible and data-poor regions. The remote sensing approach in this study highlighted the occurrence of 57 oases across the lower part of the Wenlock Basin. Bluebottle Oasis (~12.5 ha), on the Steve Irwin Wildlife Reserve, is the second largest oasis found in the lower Wenlock Basin. A remarkable concentration of 45 oases is found in the SIWR and the bauxite plateau that extends to the east of it (north of the Wenlock River). These oases of the Wenlock Basin consistently occur on the edges of the bauxite plateaus. In the terminology used to classify the springs of the Great Artesian Basin, the springs of the lower Wenlock Basin can be referred to as 'spring super-group' which describes a major regional cluster of spring-complexes with some consistent hydrogeological characteristics (Ponder, 1986; Fairfax and Fensham, 2003). Since the Cape York springs of the Wenlock Basin consistently occur on the edge of the bauxite plateau they belong to the hillslope type; although the slope angle (in average 12 degrees) is smaller than the minimum angle given in the classification system proposed by Springer and Stevens (2009).

### 5.2. Conceptual model of the springs

The stable isotope data indicate these spring waters originate from rainfall, and the $SF_6$ and CFC concentrations also indicate that recharge of these springs is not from high altitudes. The infiltration conditions with higher temperature and altitude cannot explain all measured spring data (right column in Fig. 9), whereas the

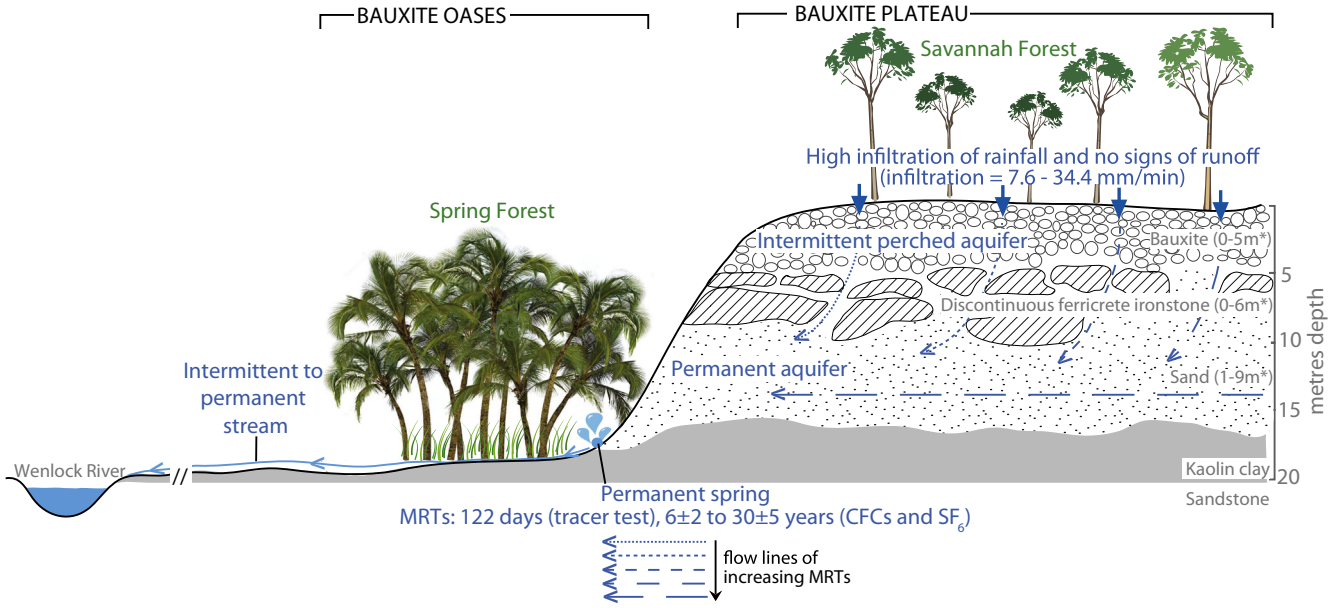


**Fig. 13.** Conceptual model of the hydrogeological functioning of the bauxite oases. ∗ range of possible values for the thickness for each geological formation compiled from 14 boreholes up to 18 m deep drilling in the Steve Irwin Wildlife Reserve. As schematically illustrated by the flow lines the springs comprise a mix of waters of different MRTs, which is the reason why no single age can explain the system and multiple data sets were required.

conditions with lower temperature and altitude create $SF_6$ and CFC concentrations high enough for all springs. We therefore conclude that at least waters of Pitcher Plant spring are probably not infiltrated in the higher and more remote mountain ranges. The most probable simple model explaining all springs is that waters are infiltrated during larger rain events creating lower soil temperatures and at an altitude of about 40 m. If CFC degradation is assumed, the infiltration conditions at 22 °C and 40 m altitude can explain all spring tracer values, but a distinction between EM or PM models would not be possible. In the PM, however, no contribution of water younger than 2 years would be possible for Oasis spring, but such a contribution is indicated by the tracer test (see below). The exponential model with a mean residence time of 14–18 years, as indicated shifting the measured values in Fig. 9c and e horizontally to the green line, would contain 5–7% water younger than 1 year. We therefore conclude that, with the very simple model assumptions here, an exponential model, representing homogeneous recharge, is the most appropriate explanation of these spring tracer findings and that the mean residence times (MRTs) according to this model range from 6 ± 2 years at Pitcher Plant spring to 30 ± 5 years at Blue Bottle spring.

The low TDS contents of the spring waters (median 35.6 mg $L^{-1}$, with a range of 27.7–72.3 mg $L^{-1}$) reflects very minor water-rock interactions and evaporation effects during rainfall recharge and subsurface flow of the spring waters. The low TDS contents of the spring waters will also reflect the short MRTs (<35 years) and/or high infiltration velocity and flow rates. In other studies of tropical savannah basins, weakly mineralised spring waters (TDS < 100 mg $L^{-1}$) have been identified in the upper catchment areas and correspond to short MRTs (e.g. McKenzie et al., 2001). The infiltration and tracer tests in this study indicate that the bauxite aquifer can provide efficient flow pathways that discharge at spring sites. The series of infiltration tests show the bauxite to have a higher field saturated hydraulic conductivity than the other land surface types found across the Steve Irwin Wildlife Reserve. This means that most of the rain falling across the bauxite surface infiltrates into the ground where it can become groundwater recharge upon reaching the water-table. In addition, the artificial tracing test demonstrates the existence of a flowpath between the bauxite surface and the sandy aquifer at Oasis Spring, and the data indicates that the groundwater velocity has a median velocity of the tracer of ~1.8 m $d^{-1}$. This bauxite aquifer may therefore play a critical role in the functioning of the springs' hydrogeological system.

This is a first conceptual model of the spring waters hydrochemistry and hydrodynamics, and these conclusions were only possible by combining multiple lines of evidence from several tracers. For example the MRTs were estimated using multiple dating tracers (CFCs and $SF_6$) coupled with information from the tracing experiment. Future work is required to compare these results with other springs in the Wenlock Basin (57 springs mapped). In addition, future assessments of wet and dry season chemical variability within the spring water would also help in the defining the hydrochemical and hydrogeological system.

### 5.3. Implications for spring management

Information on the occurrence, origin, chemistry, and hydrogeological functioning of these permanent springs is an important step to the effective management of the dependant surface water resources and ecosystems across the Wenlock Basin. For example, the role of the bauxite plateaus in the functioning of these springs is important information to consider in the context of bauxite mining. Gould (2012) showed in the Cape York Peninsula that post-mining rehabilitation of the ecosystems linked to the bauxite plateau is difficult. In addition to Cape York, bauxite mining occurs across Australia on the Darling Plateau in Western Australia and in Gove, Arnhem Land. In each region, there is a focus on post-mining rehabilitation of flora and fauna (Nichols and Gardner, 1998; Ward, 1999; Koch and Hobbs, 2007). In terms of the hydrological cycle impacts from bauxite mining, studies in Cape York are few. There have been some studies in the Darling Plateau (Croton and Reed, 2007). However, it is not possible to extrapolate results from WA to the Cape York case as regional settings (geologic, biologic and climatic), and in particular rainfall amount and intensity are very different (average annual rainfall across the Darling Plateau is below 1400 mm). The results from our study highlight a link

between the bauxite aquifer and the permanent spring systems in the lower part of the Wenlock Basin in the Cape York Peninsula. Therefore, any changes in the bauxite aquifer properties due to mining, for example due to replacement soils (e.g. Schwenke et al., 2000), can impact the physical and chemical components of the springs. The MRTs of the spring waters sampled indicate any environmental change effects at the lands surface will be observed in the spring waters within <35 years of the impact.

The findings from this research study were submited in 2013–2014 to the Queensland Parliament and its committee for the Regional Planning Interests Bill; and have, along with other evidence, contributed to the conservation of some of the oases. The Steve Irwin Wildlife Reserve on Cape York has been declared a Queensland "Strategic Environment Area". This environmental legislation aims to protect areas of regional interest from activities that risk widespread impacts to their ecological integrity.

## 6. Conclusions

The approach of using remote sensing data coupled with hydrochemistry and hydrodynamic data are able to indicate different aspects of this pristine spring system in the Cape York Peninsula. The remote sensing data is used to highlight the spring occurrence, whereas the hydrochemistry and hydrodynamics are used to highlight the origin, chemical variability, and flow pathways of the spring waters. The combined datasets provide a first conceptual hydrogeological model of the hydrodynamic and hydrochemical functioning of the study area (Fig. 13). The springs studied in detail indicate links between the spring waters with local recharge via bauxite aquifers, which promote high infiltration rates, low MRTs and retain a fresh water signature. Future work is required to refine this model, extend the analysis to include the spatial variability between the 57 springs mapped, and the seasonal variability of this model in this dry tropical region.

## References


Alfaro, C., Wallace, M., 1994. Origin and classification of springs and historical review with current applications. Environ. Geol. 24 (2), 112–124.

Arthur, C., 2009. Tephitthigghi Traditional Owner, personal communication.

Australian Bureau of Meteorology, 2014. <http://www.bom.gov.au/>. (accessed June 2014).

Bagarello, V., Iovino, M., Elrick, D., 2004. A simplified falling-head technique for rapid determination of field-saturated hydraulic conductivity. Soil Sci. Soc. Am. J. 68 (1), 66–73.

Barquín, J., Scarsbrook, M., 2008. Management and conservation strategies for coldwater springs. Aquat. Conserv.: Mar. Freshw. Ecosyst. 18 (5), 580–591.

Boulton, A.J., Hancock, P.J., 2006. Rivers as groundwater-dependent ecosystems: a review of degrees of dependency, riverine processes and management implications. Aust. J. Bot. 54 (2), 133–144.

Bryan, K., 1919. Classification of springs. J. Geol., 522–561

Cook, F.J., 2002. The twin-ring method for measuring saturated hydraulic conductivity and sorptivity in the field. In: McKenzie, N., Coughlin, K., Cresswell, H. (Eds.). Soil physical measurement and interpretation for land evaluation, pp. 108–118 (CSIRO Publishing, Melbourne).

Corsini, A., Cervi, F., Ronchetti, F., 2009. Weight of evidence and artificial neural networks for potential groundwater spring mapping: an application to the Mt. Modino area (Northern Apennines, Italy). Geomorphology 111 (1), 79–87.

CSIRO, 2009. Water in the Gulf of Carpentaria Drainage Division. A report to the Australian Government from the CSIRO Northern Australia Sustainable Yields Project. CSIRO Water for a Healthy Country Flagship, Australia, p. 479.

Crosbie, R.S., Morrow, D., Cresswell, R.G., Leaney, F.W., Lamontagne, S., Lefournour, M., 2012. New insights into the chemical and isotopic composition of rainfall across Australia. CSIRO Water for a Healthy Country Flagship, Australia.

Croton, J.T., Reed, A.J., 2007. Hydrology and bauxite mining on the darling plateau. Restor. Ecol. 15, S40–S47. http://dx.doi.org/10.1111/j.1526-100X.2007.00291.x.

Darling, W.G., Gooddy, D.C., MacDonald, A.M., Morris, B.L., 2012. The practicalities of using CFCs and $SF_6$ for groundwater dating and tracing. Appl. Geochem. 27, 1688–1697.

Department of the Environment, 2014. The community of native species dependent on natural discharge of groundwater from the Great Artesian Basin in Community and Species Profile and Threats Database, Department of the Environment, Canberra. <http://www.environment.gov.au/sprat> (accessed 10.06.14).

Domenico, P.A., Schwartz, F.W., 1990. Physical and Chemical Hydrogeology. John Wiley and Sons Inc., New York, pp. 29–41.

Drever, J.I., 1997. The geochemistry of natural waters, surface and groundwater environments, 3rd ed. In: McConnin RA (Ed.), Prentice-Hall Inc.

DWLBC, 2009. Prioritising springs of ecological significance in the Flinders Ranges. Department of Water, Government of South Australia.

Fairfax, R.J., Fensham, R.J., 2003. Great Artesian Basin springs in southern Queensland 1911–2000. Memoirs Queensl. Mus. 49, 285–293.

Fallon, S.J., Fifield, L.K., Chappell, J.M., 2010. The next chapter in radiocarbon dating at the Australian National University: status report on the single stage AMS. Nucl. Instrum. Methods Phys. Res. B 268.

Fell, DG, 2009. Flora Survey of Freshwater Spring Forests, Steve Irwin Wildlife Reserve, Cape York Peninsula, Australia. Report to Australia Zoo.

Fensham, R.J., 1998. Mound springs in the Dawson River Valley, Queensland. Vegetation-environment relations and consequences of a proposed impoundment on botanical values. Pacific Conserv. Biol. 4 (1), 42.

Fensham, R.J., Fairfax, R.J., 2003. Spring wetlands of the Great Artesian Basin, Queensland, Australia. Wetl. Ecol. Manage. 11 (5), 343–362.

Fensham, R.J., Price, R.J., 2004. Ranking spring wetlands in the Great Artesian Basin of Australian using endemnicity and isolation of plant species. Biol. Conserv. 119, 41–50.

Fensham, R.J., Fairfax, R.J., Sharpe, P.R., 2004. Spring wetlands in seasonally arid Queensland: floristics, environmental relations, classification and conservation values. Aust. J. Bot. 52 (5), 583–595.

Fensham, R.J., Ponder, W.F., Fairfax, R.J., 2010. Recovery plan for the community of native species dependent on natural discharge of groundwater from the Great Artesian Basin. Report to Department of the Environment, Water, Heritage and the Arts, Canberra. Queensland Department of Environment and Resource Management, Brisbane. <http://www.environment.gov.au/biodiversity/threatened/publications/recovery/great-artesian-basin-ec.html>.

Gao, B.C., 1996. NDWI—a normalized difference water index for remote sensing of vegetation liquid water from space. Remote Sens. Environ. 58 (3), 257–266.

Gardner, P., Solomon, D.K., 2009. An advanced passive diffusion sampler for the determination of dissolved gas concentrations. Water Resour. Res. 45 (W06423), 1–12.

Goldscheider, N., Meiman, J., Pronk, M., Smart, C., 2008. Tracer tests in karst hydrogeology and speleology. Int. J. Speleol. 37(1), 27–40 (Bologna (Italy)).

Gould, S.F., 2012. Comparison of post-mining rehabilitation with reference ecosystems in monsoonal eucalypt woodlands, Northern Australia. Restor. Ecol. 20 (2), 250–259.

Hayashi, M., Rosenberry, D.O., 2002. Effects of ground water exchange on the hydrology and ecology of surface water. Ground Water 40 (3), 309–316.

Heaton, T.H.E., Vogel, J.C., 1981. "Excess Air" in groundwater. J. Hydrol. 50, 201–216.

Howard, J., Merrifield, M., 2010. Mapping groundwater dependent ecosystems in California. PLoS ONE 5 (6), e11249.

IAEA, 2006. Use of chlorofluorocarbons in hydrology: a guidebook. Vienna, ISBN 92-0-1000805-8, 291p.

Ju, J., Roy, D.P., Vermote, E., Masek, J., Kovalskyy, V., 2012. Continental-scale validation of MODIS-based and LEDAPS Landsat ETM+ atmospheric correction methods. Remote Sens. Environ. 122, 175–184.

Kennard, M.J., Pusey, B.J., Olden, J.D., MacKay, S.J., Stein, J.L., Marsh, N., 2010. Classification of natural flow regimes in Australia to support environmental flow management. Freshw. Biol. 55 (1), 171–193.

Koch, J.M., Hobbs, R.J., 2007. Synthesis: is Alcoa successfully restoring a jarrah forest ecosystem after bauxite mining in Western Australia? Restor. Ecol. 15 (s4), S137–S144.

Kranjc (Ed.), 1997. Tracer Hydrology 97. Balkema, Rotterdam.

Langmuir, D., 1997. Aqueous environmental geochemistry, McConnin RA (Ed.).

Leibundgut, C., Maloszewski, P., Külls, C., 2009. Tracers in Hydrology. Wiley, NY.

Lewis, E., Wallace, D.W.R., 1998. Program Developed for $CO_2$ System Calculations. ORNL/CDIAC-105. Carbon Dioxide Information Analysis Center, Oak Ridge National Laboratory, U.S. Department of Energy, Oak Ridge, Tennessee.

Lyon, BJ, Franklin, C.E., 2012. Natural Values of the Bauxite Springs, Steve Irwin Wildlife Reserve, Cape York Peninsula. Report to the National Heritage Trust and Australia Zoo.

MacKay, H., 2006. Protection and management of groundwater-dependent ecosystems: emerging challenges and potential approaches for policy and management. Aust. J. Bot. 54 (2), 231–237.

Mackey, B.G., Nix, H., Hitchcock, P., 2001. The Natural Heritage Significance of Cape York Peninsula. Q.E.P. Agency, ANUTECH Pty Ltd..

McKenzie, J.M., Siegel, D.I., Patterson, W., McKenzie, D.J., 2001. A geochemical survey of spring water from the main Ethiopian rift valley, southern Ethiopia: implications for well-head protection. Hydrogeol. J. 9, 265–272.

Meinzer, O.E., 1923. Outline of Ground-Water Hydrology. US Geology Survey Water Supply, 8.

Mudd, G.M., 2000. Mound springs of the Great Artesian Basin in South Australia: a case study from Olympic Dam. Environ. Geol. 39 (5), 463–476.

Munksgaard, N.C., Wurster, C.M., Bass, A., Bird, M.I., 2012. Extreme short-term stable isotope variability revealed by continuous rainwater analysis. Hydrol. Process. http://dx.doi.org/10.1002/hyp.9505.

Nevill, J.C., Hancock, P.J., Murray, B.R., Ponder, W.F., Humphreys, W.F., Phillips, M.L., Groom, P.K., 2010. Groundwater-dependent ecosystems and the dangers of groundwater overdraft: a review and an Australian perspective. Pacific Conserv. Biol. 16 (3), 187–208.

Nichols, O.G., Gardner, J.H., 1998. Long-term monitoring of fauna return in bauxite-mined areas of the Darling Range. In: Asher, C.J., Bell, L.C. (Eds.), Proceedings of

the Fauna Habitat Reconstruction after Mining Workshop, Adelaide, 10–11 October 1997. Australian Centre for Mining Environmental Research, Brisbane, pp. 99–109.
Oh, H.J., Kim, Y.S., Choi, J.K., Park, E., Lee, S., 2011. GIS mapping of regional probabilistic groundwater potential in the area of Pohang City, Korea. J. Hydrol. 399 (3), 158–172.
Oster, H., Sonnag, C., Munnich, K.O., 1996. Groundwater age dating with chlorofluorocarbons. Water Resources Res. 37, 2989–3001.
Petus, C., Lewis, M., White, D., 2013. Monitoring temporal dynamics of Great Artesian Basin wetland vegetation, Australia, using MODIS NDVI. Ecol. Ind. 34, 41–52.
Plummer, L.N., Busenberg, E., 1999. Chlorofluorocarbons. In: Cook, P.G., Herczeg, A.L. (Eds.), Environmental Tracers in Subsurface Hydrology. Kluwer, Dordrecht, pp. 441–478.
Ponder, W.F., 1986. Mound springs of the great artesian basin. In Limnology in Australia (pp. 403–420). Springer, Netherlands.
QDEHP, 2014. Queensland Department of Environment and Heritage Protection. <https://environment.ehp.qld.gov.au/regional-ecosystems/> (last consulted January 2014).
Queensland Herbarium, 2014. <http://www.qld.gov.au/environment/plants-animals/plants/herbarium/about/> (last consulted January 2014).
Saraf, A.K., Goyal, V.C., Negi, A.S., Roy, B., Choudhary, P.R., 2000. Remote sensing and GIS techniques for the study of springs in a watershed in Garhwal in the Himalayas, India. Int. J. Rem. Sens. 21 (12), 2353–2361.
Sattler, P., Williams, R., 1999. The Conservation Status of Queensland's Bioregional Ecosystems. Environmental Protection Agency, Queensland Government.
Schulte, P., van Geldern, R., Freitag, H., Karim, A., Négrel, P., Petelet-Giraud, E., Probst, A., Probst, J.-L., Telmer, K., Veizer, J., Barth, J.A.C., 2011. Applications of stable water and carbon isotopes in watershed research: weathering, carbon cycling, and water balances. Earth Sci. Rev. 109, 20–31.
Schwenke, G.D., Ayre, L., Mulligan, D.R., Bell, L.C., 2000. Soil stripping and replacement for the rehabilitation of bauxite-mined land at Weipa. II. Soil organic matter dynamics in mine soil chronosequences. Soil Res. 38 (2), 371–394.
Sener, E., Davraz, A., Ozcelik, M., 2005. An integration of GIS and remote sensing in groundwater investigations: a case study in Burdur, Turkey. Hydrogeol. J. 13 (5–6), 826–834.
SKM and CSIRO, 2012. Atlas of Groundwater Dependent Ecosystems (GDE Atlas), Phase 2 Task 5 Report: Identifying and Mapping GDEs. N.W. Commission, Sinclair Knight Merz.
Specht, R.L., Salt, R.B., Reynolds, S.T., 1977. Vegetation in the Vicinity of Weipa, North Queensland. Proc. R. Soc. Queensl. 88, 17–38.
Springer, A.E., Stevens, L.E., 2009. Spheres of discharge of springs. Hydrogeol. J. 17 (1), 83–93.
Suckow, A., 2012. Lumpy – an interactive Lumped Parameter Modeling code based on MS Access and MS Excel. Geophysical Research Abstracts, European Geosciences Union 14.
Suckow, A., 2014. The Age of Groundwater – definitions, models and why we do not need this term. Appl. Geochem. http://dx.doi.org/10.1016/j.apgeochem.2014.04.016.
Torgersen, T., Stute, M., 2013. Helium (and other Noble Gases) as a tool for understanding long timescale groundwater transport. In: Suckow, A., Aggarwal, P.K., Araguas-Araguas, L.J. (Eds.), Isotope Methods for Dating Old Groundwater. International Atomic Energy Agency, Vienna, pp. 179–216 (chap. 8).
Valentine, P.S., Mackey, B., Hitchcock, P., 2013. The Natural Attributes for World Nomination of Cape York Peninsula, Australia. Report to the Queensland Government.
Vogel, J.C., 1967. Investigation of groundwater flow with radiocarbon. Isotopes in Hydrology, IAEA-SM-83/24, Vienna, pp. 255–368.
Ward, S.C., 1999. Assessing rehabilitation development on Alcoa's bauxite mines. In: Asher, C.J., Bell, L.C. (Eds.), Proceedings of the Workshop on Indicators of Ecosystem Rehabilitation Success, Melbourne, 23–24 October 1998. Australian Centre for Mining Environmental Research, Brisbane, pp. 91–103.
Warfe, D.M., Pettit, N.E., Davies, P.M., Pusey, B.J., Hamilton, S.K., Kennard, M.J., Townsend, S.A., Bayliss, P., Ward, D.P., Douglas, M.M., Burford, M.A., Finn, M., Bunn, S.E., Halliday, I.A., 2011. The 'wet–dry' in the wet–dry tropics drives river ecosystem structure and processes in northern Australia. Freshw. Biol. 56 (11), 2169–2195.
Willmott, W., 2009. Areas of Cape York Peninsula of International Conservation Significance. The Geological Story of Cape York Peninsula.
Wood, P.J., Hannah, D.M., Sadler, J.P., 2008. Hydroecology and Ecohydrology: Past, Present and Future. John Wiley & Sons, 28 févr. 2008, 460 pages.